Current Optics and Photonics
Vol. 2, No. 1, February 2018, pp. 53-58

ISSN: 2508-7266(Print) / ISSN: 2508-7274(Online)
DOI: https://doi.org/10.3807/COPP.2018.2.1.053

A Novel High Speed Frequency Sweeping Signal Generator in X-band Based on Tunable Optoelectronic Oscillator

Mingming Sun[1], Han Chen[2], and Xiaohan Sun[1]*

[1]*National Research Center for Optical Sensing/Communications Integrated Networking, Southeast University, Nanjing 210096, China*
[2]*School of Instrument Science and Engineering, Southeast University, Nanjing 210096, China*

(Received September 19, 2017 : revised January 17, 2018 : accepted January 19, 2018)

A novel X-band high speed frequency sweep signal generator based on a tunable optoelectronic oscillator (OEO) incorporating a frequency-swept laser is presented and the theoretical fundamentals of the design are explained. A prototype of the generator with tuning range from 8.8552 GHz to 10.3992 GHz and a fine step about 8 MHz is achieved. The generated radiofrequency signal with a single sideband (SSB) phase noise lower than -100 dBc/Hz@10KHz is experimentally demonstrated within the whole tunable range, without any narrow RF band-pass filters in the loop. And the tuning speed of the frequency sweep signal generator can reach to over 1 GHz/s benefiting from applying a novel dispersion compensation modular instead of several tens of kilometers of optical fiber delay line in the system.

Keywords : Frequency sweep, Optoelectronic oscillator, Dispersion compensation modular
OCIS codes : (060.5625) Radio frequency photonics; (230.4910) Oscillators; (250.4745) Optical processing devices

I. INTRODUCTION

With the development of electronic science and technology, frequency sweep measurement technology is increasingly valued, especially the X-band linear swept source in the test of radio communications, radio and television, radar navigation [1, 2], satellite ground stations, etc. The traditional frequency swept source is mainly based on digital frequency synthesis technology [3, 4], however, the upper limit of output frequency, 5-6 GHz in [5-7], cannot be too high and the frequency sweep range is limited.

Recently, an optoelectronic oscillator (OEO) has been used to generate a microwave signal with a high spectrum purity from 100 MHz to 100 GHz by using light wave energy storage elements, and it is considered as one of the most promising techniques for implementing a frequency sweep signal generator. Photonics and electronic techniques provide several viable solutions for realization of OEOs and their tunability [8-20], and these techniques can be classified into four categories: 1) tuning the central frequency of the RF or optical filters in loops [8, 9], 2) tuning either the wavelength of the incident light wave or the longitudinal modes of the light source in loops [10, 11], 3) tuning the chromatic dispersion values of the dispersion elements in loops such as a fiber Bragg grating (FBG) and a dispersion compensating fiber (DCF) [12, 13], 4) tuning the polarization state of the light wave in loops with a polarization controller (PC) [14]. However, those proposed schemes to implement tunable OEOs are usually costly due to the bulky components and specific operating conditions with the frequency tunable range limited to several MHz [15], and the tuning speed (GHz/s) of the oscillator is usually compromised. Furthermore, by using the tunable high-Q electrical filters, yttrium iron garnet (YIG) filter, e.g., the OEO can have a tunable range of several GHz. However, its tuning speed is relatively low, and very high and stable drive current is required [9]. Recently, phase-modulation-based single passband microwave photonic

*Corresponding author: xhsun@seu.edu.cn, ORCID 0000-0003-4645-3788
Color versions of one or more of the figures in this paper are available online.

filter (MPF) [16, 17] have attracted great attention due to the advantage of no dc bias drift for the phase modulators compared to the electrical filter. Among the MPF methods, stimulated Brillouin scattering (SBS) based MPF in an OEO can easy generate wideband frequency such as 4-16 GHz in [18] but a -45 dbc/Hz@10kHz phase noise [19] due to the amplified spontaneous emission noise (ASE).

Besides frequency tunability, several architectures for constructing multiloop OEOs have been realized to improve the phase stability. X. S. Yao [20] demonstrated dual-loop OEOs incorporating two separated fiber delay lines with unequal lengths, and much work has been carried out [21, 22]. J. Yang [23] proposed a polarization-beam splitter/combiner based dual-loop scheme, and S. Pan [24] also demonstrated the scheme incorporating a polarization modulator. F. Kong [25] demonstrated a dual-frequency OEO incorporating a phase-shifted fiber Bragg grating (FBG) fabricated using a polarization maintaining fiber. More importantly, the frequency tunability would be complicated and the tunable range is as small as only a few MHz if a multiple-loop structure is employed. Among all the above methods, most efforts focused on the optical fiber loop structure design, which works as a feedback microwave ring cavity, and results show the increase of cavity length is helpful for suppressing single sideband (SSB) phase noise. However, the following factors limit the increase of cavity length: 1) longer fiber loop means more sensitive to environmental perturbations, such as temperature and vibration; 2) longer fiber loop means more oscillation modes need to be suppressed by a more effective narrowband optical filter; 3) longer fiber loop means slower tuning speed.

In this paper, we demonstrate a sweeping frequency signal generator based on a tunable optoelectronic oscillator incorporating a frequency-swept laser. The tunable microwave signal ranges from 8.8552 GHz to 10.3992 GHz in X-band with a fine step about 8 MHz, and the tuning speed can exceed 1 GHz/s. A prototype of the OEO with a frequency of 9.1992 GHz and 10.3992 GHz is experimentally demonstrated. The generated radiofrequency signal exhibits a good stability with a single sideband phase noise lower than -100 dBc/Hz at an offset of 10 KHz within the whole tunable range, without any narrow electric RF bandpass filters in the loop.

II. EXPERIMENTAL SETUP

The scheme used to experimentally demonstrate the X-band high speed sweeping frequency signal generator is shown in Fig. 1. A frequency-swept laser (Agilent 81600B) tuned from 1527.60 nm to 1565.50 nm is used as the optical source. The light wave from the laser is modulated by the feedback electrical signal via a phase modulator (PM). The amplitude of the optical signal is controlled by an erbium doped fiber amplifier (EDFA) and a variable

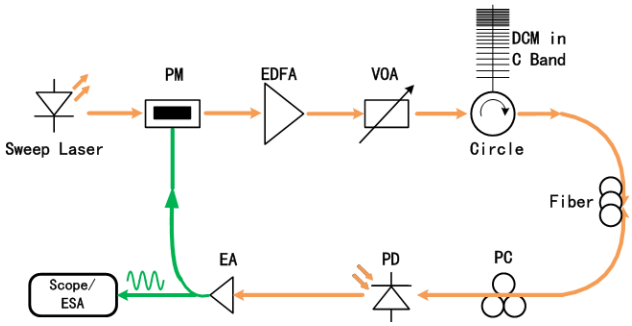

FIG. 1. Experimental setup for the X-band high speed sweeping frequency signal generator based on a tunable OEO.

optical attenuator (VOA). Then the modulated signal is sent to a dispersion compensation module (DCM) in C band via an optical circulator. The compensated residual dispersion in the system depends on the laser central wavelength, that determines the generated frequency of the OEO. After that, the optical signal is sent to a polarization controller (PC) and received by a photoelectric detector (PD). Finally, the electrical signal is sent back to the PM to close the OEO loop. An electronic amplifier (EA) is also incorporated to ensure the loop gain is higher than unity.

In addition, the proposed scheme incorporating a DCM substitute for the traditional optical delay line, which shortens the entire loop to about 20 m compared with the 50 km mentioned above. The DCM is a chirp Bragg grating in C-band by the Proximion Company, which can compensate a G.652 optical fiber dispersion up to 240 km and a G. 655 optical fiber dispersion up to 480 km with a loss less than 8 dB.

III. PRINCIPLE

Assume the PM is driven by an RF feedback signal $V_e \cdot cos\omega_e t$, where V_e is the amplitude and ω_e is the angular frequency of the RF feedback signal,.. For convenience, the electrical field $E_1(t)$ at the output of the PM can be expressed as

$$E_1(t) = E_0 \cdot \exp\left\{ j\left[\omega_0 t + \frac{V_e}{V_\pi}\cos(\omega_e t) \right] \right\} = E_0 \cdot \exp(j\omega_0 t) \sum_{n=-\infty}^{\infty} j^n \cdot J_n(\gamma) \cdot \exp(jn\omega_e t) \quad (1)$$

where E_0 and ω_0 are the amplitude and angular frequency of the incident light wave, J_n is the nth-order Bessel function of the first kind, $\gamma = V_e / V_\pi$ is the phase modulation index and V_π is the half wave voltage of the PM. In the case of small signal modulation, the above Eq. (1) can be rewritten as

$$E_1(t) \approx E_0 \left[\begin{array}{c} J_0(\gamma)\cdot\cos(\omega_0 t) + J_1(\gamma)\cdot\cos\left(\omega_0 t + \omega_e t + \frac{\pi}{2}\right) \\ -J_1(\gamma)\cdot\cos\left(\omega_0 t - \omega_e t - \frac{\pi}{2}\right) \end{array} \right] \tag{2}$$

Following that, the modulated signal is sent to a DCM via an optical circulator, and the X-band oscillation frequency is achieved by the optoelectronic oscillator loop. Finally, the microwave signal is detected by a PD and can be expressed as [12]

$$\begin{aligned} V'(\omega_e,t) &= \exp(j\omega_e t)\cdot\sum_{m=0}^{\infty}\left\{A\cdot G\cdot J_0\left[\gamma'(\omega_E)\right]J_1\left[\gamma'(\omega_e)\right]\cdot\cos\left(\frac{\chi\lambda^2\omega_e^2}{4\pi c}+\frac{\pi}{2}\right)\right\}^m \\ &\quad\cdot\exp\left(j\omega_e\frac{n_0 L}{c}\right) \\ &= \exp(j\omega_e t)\cdot\sum_{m=0}^{\infty}\left[G_{eff}(\omega_e)\right]^m\cdot\exp\left(jm\omega_e\frac{n_0 L}{c}\right) \end{aligned} \tag{3}$$

where A is a constant influenced by the optical fiber loss and response of the photodetector, n_0 is the optical fiber refractive index, λ is the wavelength of the swept wavelength tunable laser, G is the gain provided by the EA, L is the equivalent length of DCM, χ is the dispersion value of the DCM, and

$$\gamma'(\omega_e) = 2V_e\cos(\omega_e\tau/2)/V_\pi \tag{4}$$

G_{eff} is the effective open loop gain, given by

$$G_{eff}(\omega_e) = A\cdot G\cdot J_0\left[\gamma'(\omega_e)\right]J_1\left[\gamma'(\omega_e)\right]\cos\left(\frac{\chi\lambda^2\omega_e^2}{4\pi c}+\frac{\pi}{2}\right) \tag{5}$$

When the effective open-loop gain G_{eff} is less than unity, Eq. (3) can be simplified to

$$V'(\omega_e,t) \propto \frac{\exp(jw_e t)}{1-G_{eff}(\omega_e)\cdot\exp\left(j\omega_e\frac{n_0 L}{c}\right)} \tag{6}$$

The corresponding microwave power $P(\omega_e,t)$ is then given by

$$P(\omega_e,t) \propto \frac{1}{1+G_{eff}^2(\omega_e)-2G_{eff}(\omega_e)\cdot\cos\left(\omega_e\frac{n_0 L}{c}\right)} \tag{7}$$

When the OEO loop parameter meets the condition as follows:

$$\omega_e = \omega_{OSC} = \frac{\pi}{\lambda}\sqrt{\frac{2c}{\chi}} \tag{8}$$

$$\omega_e = \omega_{osc} = k\cdot\frac{c}{n_0 L} \qquad (k=1,2,3...) \tag{9}$$

$\left|G_{eff}(\omega_\varepsilon)\right|$ will reach a maximum value and the oscillation mode with a frequency ω_{osc} will increase in phase after circulation. Therefore, ω_{osc} would be the oscillation frequency. Substituting Eq. (7) to Eq. (6) yields

$$P(\omega_{OSC},t) \propto \frac{1}{\left[1-G_{eff}(\omega_{OSC})\right]^2} \tag{10}$$

When $\lambda = 1527.6\,nm$, $\chi = 593\,ps/nm$, we get $f_{osc} = 10.399\,GHz$ and when $\lambda = 1565.5\,nm$, $\chi = 779\,ps/nm$, we get $f_{osc} = 8.855\,GHz$.

We can infer the microwave-signal frequency interval $\Delta\omega_{osc}$ based on Eq. (7) as

$$\Delta\omega_{osc} = -\frac{\pi}{\lambda}\sqrt{\frac{2c}{\chi}}\cdot\frac{\Delta\lambda}{\lambda} - \frac{\pi}{2\lambda}\sqrt{\frac{2c}{\chi}}\cdot\frac{\Delta\chi}{\chi} \tag{11}$$

where $\Delta\lambda$ is the wavelength interval of the frequency-swept laser, $\Delta\chi$ is the dispersion variation introduced by wavelength dependence of the DCM.

IV. RESULTS AND DISCUSSION

In this experiment, we use an Agilent 81600B as a swept laser source tuned from 1527.60 nm to 1565.50 nm linearly with a wavelength scanning speed of 80 nm/s and a wavelength resolution of 0.2 nm, which has an excellent absolute wavelength accuracy in ±3.6 pm and a wavelength stability in ±1 pm at 24 hours at the full wavelength range. Also a chirped fiber Bragg grating by the Provision Company is utilized as a dispersion compensation module, which can compensate the dispersion of 240 km G.652 fiber or 480 km G.655 fiber with a loss less than 8 dB.

In this experiment, the wavelength is tuned from 1525-1570 nm, in which the variation of the wavelength is a small number compared to the wavelength itself, so the relationship between the oscillation RF frequency and laser wavelength by the Eq. (8) follows approximately to the linear expression. Figure 2 consists of many experimental data points of 0.2 nm space at x axis which is more like a straight line. We choose the experimental data at 1545-1550 nm to zoom in which shows a linear curve fitting in the upper right corner of Fig. 2. The jitter of data is due to the impact of external environment on the system. The oscillation frequency decreases when the value of is increased which experimentally verifies the calculating formula above. When

FIG. 2. Measured and fitted signal frequency as a function of frequency-swept laser central wavelength.

the swept laser sweeps from 1527.60 nm to 1565.50 nm in C band, the output microwave signal in X band is achieved by the OEO which scans from 10.3992 GHz to 8.8552 GHz.

Figure 3 illustrates the corresponding observed electrical spectra of the oscillation frequencies at the output. A set of regular oscillation frequencies at X-band range from 8.8552 GHz to 10.3992 GHz of a fine step of 8 MHz which is determined by the wavelength interval The oscillations were generated satisfying the condition for a certain swept laser central wavelength.

Figure 4 shows the generated 9.1992/9.2080 GHz oscillation signal with an alternating swept laser central wavelength at 1554 nm, and the inset shows the zoom RF signal in the color grade scale persistence mode compared with the result by a 1553 nm central wavelength. Within a time of 500 μs, the proposed OEO successfully generates 8.8/8.7 GHz oscillation signals, which benefit from the short loop length of 20 m. So the tuning speed over 1

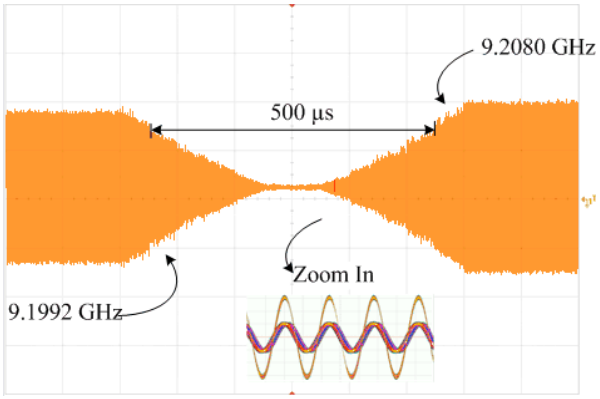

FIG. 4. Measured the generated 9.1992/9.2080 GHz oscillation signal.

GHz/s is decided by the wavelength scanning speed of Agilent 81600B with a tuning time of 0.2 nm/(80 nm/s) in one wavelength interval which is much longer than the oscillation time 500 μs.

Figure 5 shows the measured electrical spectrum and phase noise of the generated oscillation signal of 9.1992 GHz in (a) and 10.3992 GHz in (b). Respectively, when the sweep laser wavelength is 1556.96 nm, microwave signal with a center frequency of 9.19920 GHz and a phase noise of -103.2 dBc/Hz @ 10 KHz is shown in Fig. 5(a), and when the sweep laser wavelength is 1527.60 nm, microwave signal with a center frequency of 10.39920 GHz and a phase noise of -100.4 dBc/Hz @ 10 KHz is shown in Fig. 5(b). A zoom-in view of the electrical spectrum of the oscillation signal at SPAN 100 MHz and RBW 910 kHz is also provided. Results show the side mode suppression ratio is greater than 60 dB and the phase noise is about -100 dBc/Hz @ 10 KHz. Under the conditions of laboratory environment, the stability of the generated signal is evaluated and results show no mode hopping during more than an hour observation.

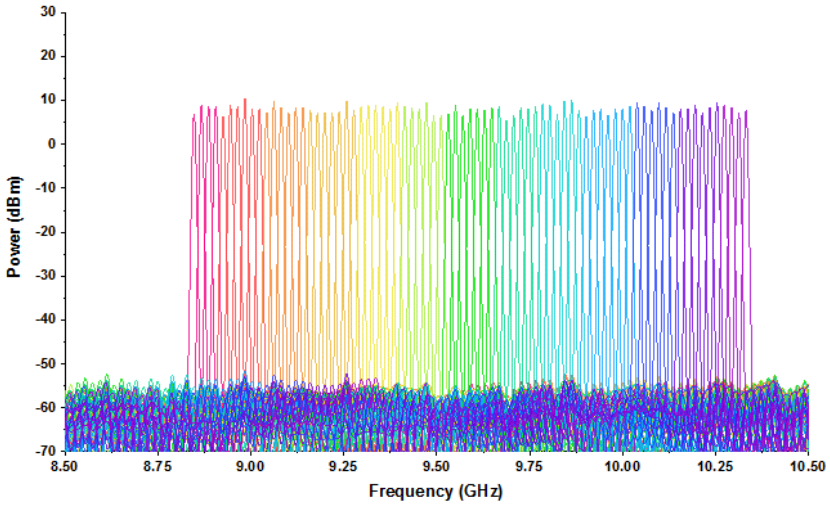

FIG. 3. Measured electrical spectra from 8.8552 GHz to 10.3992 GHz.

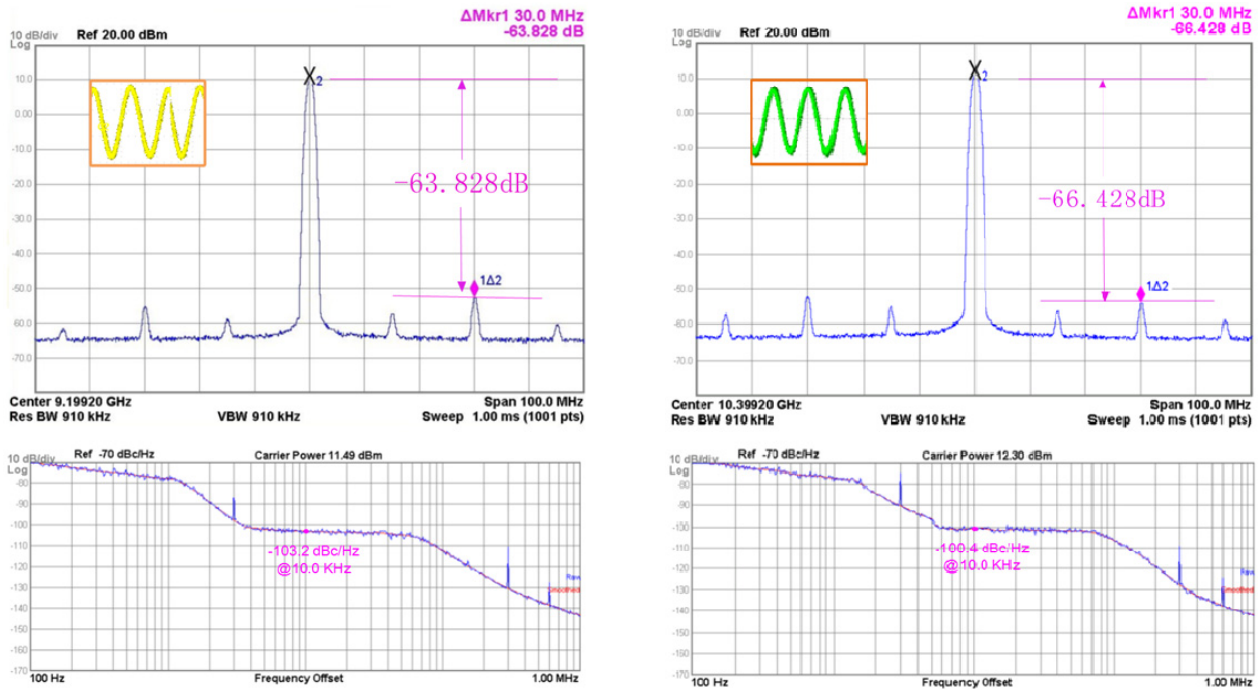

(a) (b)

FIG. 5. Measured electrical spectrum and phase noise of the generated 9.1992 GHz (a) and 10.3992 GHz (b) oscillation signal with a frequency span of 100 MHz and resolution bandwidth of 910 KHz.

V. CONCLUSION

To conclude, we presented a frequency sweep signal generator based on a tunable optoelectronic oscillator incorporating a frequency-swept laser. A prototype of the generator with tuning range from 8.8552 GHz to 10.3992 GHz and a fine step about 8 MHz is achieved. The proposed device operates at up to X-band with an SSB phase noise lower than -100 dBc/Hz is experimentally demonstrated within the whole tunable range. Besides applying a novel DCM instead of several tens of kilometers optical fiber delay line, the tuning speed can reach to over 1 GHz/s. Furthermore, if the VOA, optical amplifier, polarizer and other components are realized monolithically, the scheme allows on-chip integration while enhancing the filtering stability and lowering the manufacturing costs.

ACKNOWLEDGEMENT

This work was supported by the National Natural Science Foundation of China (No.61471116, No.61101019).

REFERENCES

1. Y. W. Huang, T. F. Tseng, C. C. Kuo, Y. J. Hwang, and C. K. Sun, "Fiber-based swept-source terahertz radar," Opt. Lett. **35**, 1344-1346 (2010).
2. S. Roehr, P. Gulden, and M. Vossiek, "Method for high precision clock synchronization in wireless systems with application to radio navigation," IEEE Radio Wireless Symp. **7**, 551-554 (2007).
3. H. C. Yeoh, J. H. Jung, Y. H. Jung, and K. H. Baek, "A 1.3-GHz 350-mW hybrid direct digital frequency synthesizer in 90-nm CMOS," IEEE J. Solid-State Circuits **45**(9), 1845-1855 (2010).
4. A. Ashrafi, R. Adhami, and A. Milenkovic, "A direct digital frequency synthesizer based on the quasi-linear interpolation method," IEEE Trans. Circuits Syst. I: Regular Papers **57**(4), 863-872 (2010).
5. S. Thuries, É. Tournier, A. Cathelin, S. Godet, and J. Graffeuil, "A 6-GHz Low-Power BiCMOS SiGe: C 0.25 µm Direct Digital Synthesizer," IEEE Microw. Wireless Compon. Lett. **18**, 46-48 (2008).
6. C. Y. Yang, J. H. Weng, and H. Y. Chang, "A 5-GHz direct digital frequency synthesizer using an analog-sine-mapping technique in 0.35-m SiGe BiCMOS," IEEE J. Solid-State Circuits **46**, 2064-2072 (2011).
7. A. Grama and G. Muntean, "Direct digital frequency synthesis implemented on a FPGA chip," in *2006 29th International Spring Seminar on Electronics Technology* (2006), pp. 92-97.
8. X. Xie, C. Zhang, T. Sun, P. Guo, X. Zhu, L. X. Zhu, W. Hu, and Z. Chen, "Wideband tunable optoelectronic oscillator based on a phase modulator and a tunable optical filter," Opt. Lett. **38**, 655-657 (2013).
9. D. Zhu, S. Pan, and D. Ben, "Tunable frequency-quadrupling dual-loop optoelectronic oscillator," IEEE Photon. Technol. Lett. **24**, 194-196 (2012).
10. S. Pan and J. P. Yao, "Wideband and frequency-tunable microwave generation using an optoelectronic oscillator

incorporating a Fabry-Perot laser diode with external optical injection," Opt. Lett. **35**, 1911-1913 (2010).
11. W. Li and J. P. Yao, "A wideband frequency-tunable optoelectronic oscillator incorporating a tunable microwave-photonic filter based on phase-modulation to intensity-modulation conversion using a phase-shifted fiber Bragg grating," IEEE Trans. Microw. Theory Techn. **60**, 1735-1742 (2012).
12. M. Li, W. Li, and J. P. Yao, Tunable optoelectronic oscillator incorporating a high-Q spectrum-sliced photonic microwave transversal filter," IEEE Photon. Technol. Lett. **24**, 1251-1253 (2012).
13. W. Li and J. P. Yao, "An optically tunable optoelectronic oscillator," J. Lightw. Technol. **28**, 2640-2645 (2010).
14. Z. Tang, S. Pan, D. Zhu, R. Guo, Y. Zhao, M. Pan, D. Ben, and J. P. Yao, "Tunable optoelectronic oscillator based on a polarization modulator and a chirped FBG," IEEE Photon. Technol. Lett. **24**, 1487-1489 (2012).
15. B. Yang, X. F. Jin, H. Chi, X. M. Zhang, S. L. Zheng, S. H. Zou, K. S. Chen, E. Tangdiongga, and T. Koonen, "Optically tunable frequency-doubling Brillouin optoelectronic oscillator with carrier phase-shifted double sideband modulation," Photon. Technol. Lett. **24**, 1051-1053 (2012).
16. X. Xie, C. Zhang, T. Sun, P. Guo, X. Zhu, L. Zhu, W. Hu, and Z. Chen, "Wideband tunable optoelectronic oscillator based on a phase modulator and a tunable optical filter," Opt. Lett. **38**, 655-657 (2013).
17. J. Zhang, L. Gao, and J. P. Yao, "Tunable optoelectronic oscillator incorporating a single passband microwave photonic filter," IEEE Photon. Technol. Lett. **26**, 326-329 (2014).
18. R. Tao, X. Feng, Y. Cao, Z. Li, and B. Guan, "Widely tunable single bandpass microwave photonic filter based on phase modulation and stimulated Brillouin scattering," IEEE Photon. Technol. Lett. **24**, 1097-1099 (2012).
19. X. Han, L. Ma, Y. Shao, Q. Ye, Y. Gu, and M. Zhao, "Polarization multiplexed dual-loop optoelectronic oscillator based on stimulated Brillouin scattering," Opt. Commun. **383**, 138-143 (2017).
20. X. S. Yao and L. Maleki, "Multi-loop optoelectronic oscillator," IEEE J. Quant. Electron. **36**, 79-84 (2000).
21. T. Sakamoto, T. Kawanishi, S. Shinada, and M. Izutsu, "Optoelectronic oscillator using LiNbO intensity modulator with resonant electrode," Electron. Lett. **41**, 716-718 (2005).
22. E. Shumakher and G. Eisenstein, "Noise properties of mutually sustained microwave-optoelectronic oscillator pair," Electron. Lett. **41**, 768-770 (2005).
23. Y. Jiang, J. L. Yu, Y. T. Wang, L. T. Zhang, and E. Z. Yang, "An optical domain combined dual-loop optoelectronic oscillator, IEEE Photon. Technol. Lett. **19**, 807-809 (2007).
24. S. Pan and J. P. Yao, A frequency-doubling optoelectronic oscillator using a polarization modulator," IEEE Photon. Technol. Lett. **21**, 929-931 (2009).
25. F. Kong, W. Li, and J. P. Yao, "Transverse load sensing based on a dual-frequency optoelectronic oscillator," Opt. Lett. **38**, 2611-2613 (2013).